

# The Experiment Analysis of Bonding Performance between Near Surface Mounted CFRP Strip and Concrete at Different Curing Temperatures

Zewen Zhu<sup>1</sup> · Eryu Zhu<sup>1</sup> · Zhuo Chen<sup>2</sup>

Received: 8 August 2017 / Revised: 17 July 2018 / Accepted: 5 August 2018 / Published online: 22 August 2018  
© The Author(s) 2018

**Abstract** To investigate the bonding performance of near-surface mounted (NSM) carbon fiber-reinforced polymer (CFRP) technique under different curing temperatures, a total of five test specimens strengthened with NSM CFRP strip were tested by direct pull-out methods. The strain of CFRP strip, interfacial bonding shear stress, ultimate load and failure mode were analyzed through the test. The experiment results showed that the ultimate load and bonding shear stress of the specimens increased gradually when curing temperature was lower than the glass transition temperature ( $T_g$ ) of the bond material. Afterward, they gradually decreased with the increase in temperature. The bonding shear stress was gradually transmitted from the loading end to the free end. The failure modes were changed from CFRP strip–adhesive interface bonding failure to CFRP strips fracture failure with the temperature rising. In this paper, the bonding performance experiment results of NSM CFRP strip could provide a reference for the rapid strengthening of monorail traffic track beams.

**Keywords** NSM technique · Bonding performance · CFRP strip · Concrete · Curing temperature

## 1 Introduction

Nowadays, monorail traffic has got widespread attention due to its low noise and adaptability to complex geological environment. However, when the track beam of monorail traffic suffers damages, it should be strengthened rapidly so as not to affect the normal operation of the monorail vehicle. In view of the special function and construction of the track beam, it is necessary to strengthen it with near-surface mounted (NSM) technique, which will not change the size of the original structure. The preferred reinforcement material of NSM technique is carbon fiber-reinforced polymer (CFRP) because of its lightweight, high strength, corrosion resistance and convenient construction. In order to achieve the purpose of rapid strengthening, the most effective method is to increase the cure temperature of the test specimen so as to improve the solidification rate of the adhesive material. Therefore, the bonding performance of NSM CFRP technique is more worthy of attention when the curing temperature of adhesive materials is elevated.

So far, a large number of research results show that the reinforced concrete (RC) beam strengthened with NSM technique exhibits good flexural performance at ambient condition [1, 2]. In addition, many researchers made in-depth studies of bonding performance between NSM CFRP and concrete interface at ambient condition. The main parameters affecting the bonding performance are the groove size, concrete strength, bonded length, distance from the concrete edge, adhesive type, CFRP strip size and so on [3–7]. The bonding performance between NSM CFRP and concrete has been studied fully at ambient

---

✉ Eryu Zhu  
zhu\_teacher@126.com  
Zewen Zhu  
14115294@bjtu.edu.cn  
Zhuo Chen  
chenzhuo8832@126.com

<sup>1</sup> School of Civil Engineering, Beijing Jiaotong University, No.3, Shangyuan Village, Haidian District, Beijing, China

<sup>2</sup> China Railway Fifth Survey and Design Institute Group CO., LTD, No.4, Kangzhuang Road, Huangcun Town, Daxing District, Beijing, China

conditions. However, there are few research results on the effect of temperature on the bonding performance between NSM CFRP and concrete. For example, Hu [8, 9] investigated the bonding performance between NSM CFRP and concrete at temperature range of 4–180 °C. The results show that there was a glass transition temperature of bonding material. Glass transition temperature is a watershed that affects the performance of bonding materials. Lee [10] studied the bonding properties of three kinds of filling materials (epoxy mortar EM, anti-shrink mortar NM and epoxy putty EP) subjected to 100 times temperature cycle (–15 to 55 °C). Mohammed [11] investigated the bond performance of NSM CFRP using the high-strength self-compacting cement base with graphene oxide (IHSSC-CA) as a filling material that was subjected to 400, 600, 700 and 800 °C. Yu B investigated the strength and stiffness properties of NSM CFRP through the single shear pull-out test when the specimens were subjected to 100, 200, 300 and 400 °C. The results showed that the bond strength was, respectively, reduced by 80% and 100% compared to that of the specimens in room temperature when the specimens were heated to 200 °C and 400 °C [12].

At present, the research results of the effect of curing temperature on the bond performance of NSM CFRP were not sufficient. In this paper, the direct pull-out tests of NSM CFRP applied for the concrete block were carried out by considering the effect of curing temperature. The research contents include pull-out load, bonding shear stress, local bond–slip and failure mode. The research results would lay a foundation for using NSM CFRP in rapid reinforcement of monorail track beam.

### 1.1 Experimental Design

#### (1) The test plan

To investigate the bonding performance of NSM CFRP technique applied to concrete block under different curing temperatures, a total of five direct pull-out specimens were carried out considering the effect of curing temperature. Curing temperature of the specimen was ranged from 35 to 65 °C, and curing time was constant at 12 h based on consideration of ambient temperature and adhesive allowable temperature. The dimension of the concrete block was 150 mm (width) × 150 mm (height) × 300 mm (length). The dimension of the CFRP strip was 20 mm (width) × 1.4 mm (thickness) × 400 mm (length), and the bonded length of CFRP was 200 mm. The dimension of the groove was 15 mm (width) × 30 mm (depth). The specific form of specimen is shown in Fig. 1. CFRP and epoxy were provided by Carbon Composites (Tianjin) Co., Ltd. The specific test plan is given in Table 1.

#### (2) Material properties

The concrete grade of the specimens was C50, and concrete cube compressive strength was 50.12 MPa on 28 days. The concrete elastic modulus was  $3.45 \times 10^4$  MPa, and temperature expansion coefficient of the concrete was  $10.2 \times 10^{-6} \text{ }^\circ\text{C}^{-1}$ . The ultimate tensile strength of CFRP was 2000 MPa, and its elastic modulus was 140 GPa. Temperature expansion coefficient of CFRP was  $0.3 \times 10^{-6} \text{ }^\circ\text{C}^{-1}$ . The density of epoxy resin was 1.6 g/cm<sup>3</sup>, and its tensile strength was 40 MPa. The specific material properties are given in Table 2.

#### (3) Preparation process of specimen

Preparation process of specimen includes four steps. First, the groove was injected with epoxy resin close to one-third of its depth. Second, the CFRP strip with strain gauge was embedded into the groove along the centerline of the groove (Fig. 2). Third, the remaining space continued to fill with epoxy. Fourth, the CFRP strip was lightly pressed and the overflow epoxy was removed with a spatula. Finally, the specimen was cured for a predetermined time at a set curing temperature, and the curing temperature was adjusted by an infrared heating lamp (Fig. 3).

### 1.2 Measuring Point Arrangement and Test Loading

In order to measure the strain value of CFRP during loading, five strain gauges were arranged at an unequal spacing on the CFRP strip. In order to avoid direct contact between the strain gauge and the epoxy resin, the paraffin was pasted on the strain gauge. Two linear variable differential transformers (LVDT) with a measuring range of 50 mm were arranged on the loading end and free end of the tested CFRP, respectively. Strain and displacement data were collected from the XL2118C force and strain integrated parameter tester. The specific layout position is shown in Fig. 4.

After the specimen was cured for a predetermined time, it was conducted on the pull-out test immediately using hydraulic universal testing machine with a capacity of 1000 kN (shown in Fig. 5). To prevent eccentric loading, a horizontal detector was used to monitor the loading device. The graded loading system was strictly enforced during the tests in order to observe the test phenomenon. The test loading process was described as follows.

First, in order to check the stability of the test device, it is necessary to preload on CFRP with 1 kN. During preloading, the loading device and test instrument need to be carefully checked. Second, the test specimens are loaded to half of the theoretical ultimate load at every grade 1 kN and then are loaded continuously at every grade 0.5 kN

**Fig. 1** Schematic of specimen. **a** Single shear pull-out specimen, **b** dimension of specimen

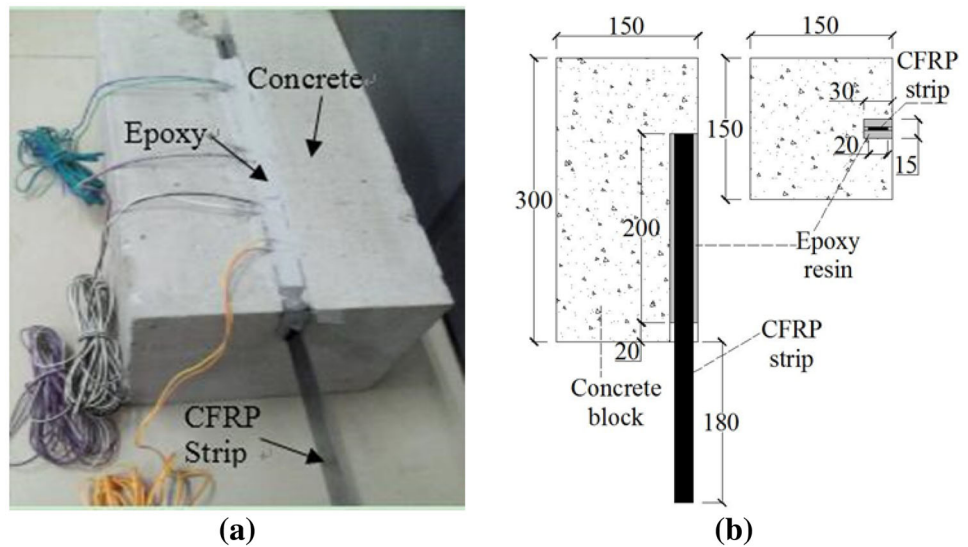


**Table 1** Test plan of NSM CFRP strip at different curing temperatures

Specimen ID	Curing temperature (°C)	Curing time (h)	Bonded length (mm)	Dimension of groove	Dimension of CFRP strip
T35	35	12	200	15 mm (width) × 30 mm (depth)	20 mm (width) × 1.4 mm (thickness)
T40	40	12			
T50	50	12			
T60	60	12			
T65	65	12			

**Table 2** Properties of test materials

Type	Test items	Technical value
CFRP plate	Tensile strength (MPa)	2000
	Elastic modulus (GPa)	$1.4 \times 10^2$
	Thickness (mm)	1.4
	Temperature expansion coefficient (°C <sup>-1</sup> )	$0.3 \times 10^{-6}$
Epoxy resin	Tensile strength (MPa)	40
	Tensile elastic modulus (MPa)	2500
	Temperature expansion coefficient (°C <sup>-1</sup> )	$55 \sim 60 \times 10^{-6}$
	Density (g/cm <sup>3</sup> )	1.6
Concrete	Measured compressive strength (MPa)	50.12
	Elastic modulus (MPa)	$3.45 \times 10^4$
	Temperature expansion coefficient (°C <sup>-1</sup> )	$10.2 \times 10^{-6}$

until the CFRP strip was pulled out. After each grade load is loaded, the load should be stabilized for 3 min. When the test data become stable, the displacement and strain data were collected, and the experiment phenomenon is observed and recorded. Data collection machine is shown in Fig. 6.

## 2 Data Processing and Results Analysis

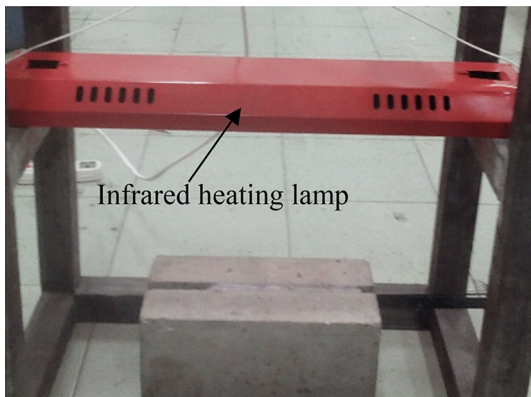
### 2.1 Data Processing

Figure 4 shows that the free end is defined as the origin of the coordinate  $X$ . The corresponding strain is  $\zeta(x_i)$  at the location of  $x_i$ . According to the relation between the interface bonding shear stress and strain in the literature

**Fig. 2** Embedded CFRP strip into the groove



**Fig. 5** Pulling out test equipment



**Fig. 3** Heated the specimen with the infrared heating lamp

[13], the bonding shear stress  $\tau(x)$  of CFRP strip can be expressed:

$$\tau\left(\frac{x_i + x_{i+1}}{2}\right) = \frac{b_h}{2} E_{cf} \frac{\xi(x_{i+1}) - \xi(x_i)}{x_{i+1} - x_i} \quad i = 1, 2, \dots, \quad (1)$$

where  $b_h$  is the thickness of CFRP strip;  $E_{cf}$  is the elastic modulus of CFRP strip;  $x_i$  is the location of strain gauge.

The slip  $u(x)$  of CFRP strip can be attained:

$$u(x_i) = u_0 + \sum_{j=1}^i \varepsilon(x_j)(x_j - x_{j-1}), \quad (2)$$

$$u\left(\frac{x_i + x_{i+1}}{2}\right) = \frac{u(x_i) + u(x_{i+1})}{2}, \quad (3)$$

where  $u_0$  is the displacement of CFRP strip at the free end.

### 2.2 Results Analysis of Bonding Performance Between NSM CFRP and Concrete

The free end of T35 specimen began to slip at the pulling load of 15 kN, and then, the CFRP strip occurred torn sound when load increased to 24 kN. Finally, the interface between adhesive and CFRP strip was destroyed due to bonding failure at 25.2 kN (shown in Fig. 7a). Because no cracks were observed on the outer surface of the specimen, the failure was speculated occurring at the interface of the CFRP–adhesive. The failure mode of T40 specimen was the interface destruction of CFRP and adhesive accompanied by adhesive cracking (shown in Fig. 7b), and the final failure load was 29.5 kN. The failure modes of T50, T60 and T65 specimens were mainly broken on CFRP strip accompanied by crack of the adhesive layer. The ultimate load was 37.1 kN, 36.3 kN and 35.2 kN, respectively.

**Fig. 4** Location of strain gauges on CFRP strip surface points 1, 2...5 (unit: mm)

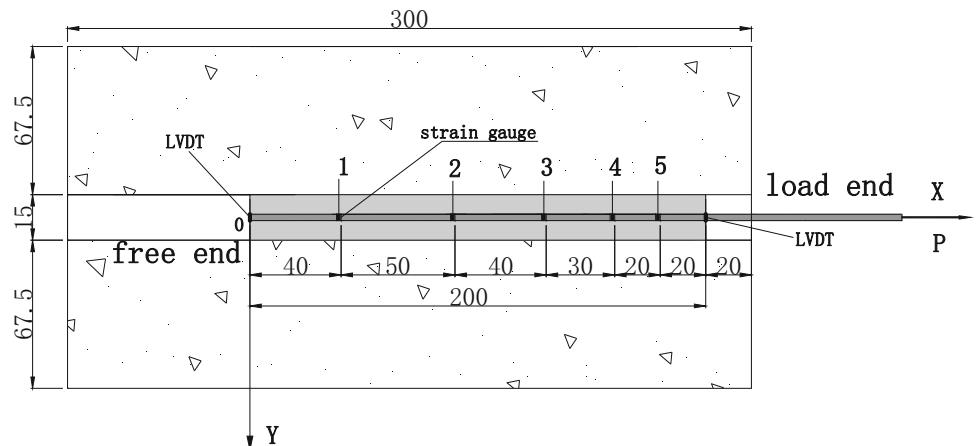




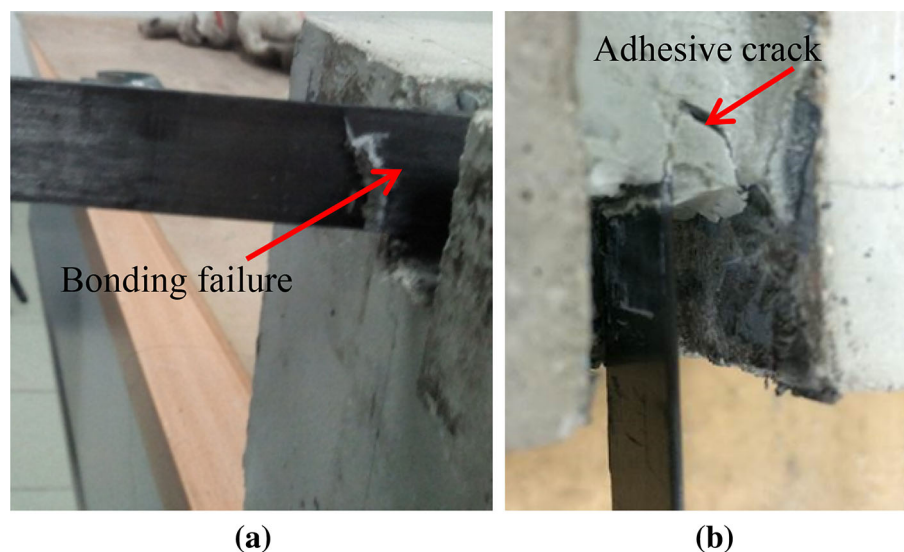


**Fig. 6** Data collection equipment

About the experiment phenomenon of T50 specimen, a crisp sound was heard when the specimen was loaded to 18.2 kN, and the sound continued to appear at 23.9 kN. It was found that there were a crack at the loading end adhesive and precipitation of a small amount of white powder. It continued to be loaded to 35 kN accompanied by the sound of the CFRP strips torn. At this time, the load increased slowly, the loading end slip increased obviously and the free end began to slip. The precipitation of white powder increased at the interface between the adhesive and CFRP. Finally, the CFRP strip was broken and a number of fine cracks appeared at 37.1 kN.

As it is given in Table 3, first, with the increase in curing temperature, the failure modes of the specimen were changed from bond failure to the fracture of the CFRP strip. Second, when curing temperature was less than 50 °C, the ultimate load increased gradually, which was increased by 47.2% from 35 to 50 °C. When curing temperature exceeded 50 °C, the ultimate load decreased gradually, which was reduced by 5% from 50 to 65 °C. The

**Fig. 7** Failure modes of specimen. **a** CFRP–adhesive bond failure, **b** adhesive crack



ultimate load tended to first increase, and then decrease with the increase in curing temperature. The ultimate load reached the maximum value 37.1 kN when curing temperature was 50 °C.

Figure 8 shows the strain distribution of CFRP strip (specimen T40). As it is shown in the figure, when the load is lower than 24 kN, the effective transfer length of strain is 110 mm. When the specimen is loaded to 29.5 kN, the free end of CFRP begins to occur strain, which indicates the effective length of strain extends to the entire bonding area of CFRP strip. With the increase in external load, the strain of CFRP gradually develops from the loading end to the free end. Figure 9 represents the strain distribution of CFRP strip (specimen T50). Compared with the strain distribution of the test specimen T40, the strain distribution of the test specimen T50 is relatively full with the increase in load.

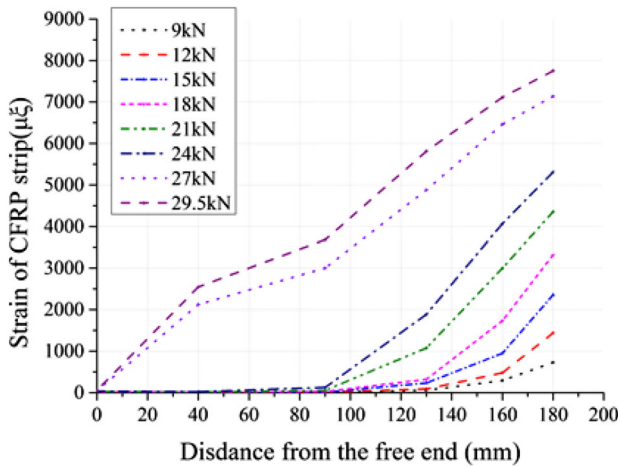
Figure 10 shows bond–slip curve of NSM CFRP strip at the different positions (specimen T60). As it is shown in the figure, the bonding shear stress reaches a peak value 8.45 MPa at the location of  $x = 170$  mm, and the slip value is 220.23  $\mu\text{m}$ . With the increase in external load, the peak shear stress is transmitted to the free end. At the location of  $x = 145$  mm, the peak bonding shear stress reaches 8.02 MPa, and the slip value is 809.7  $\mu\text{m}$ . At the location of  $x = 110$  mm and 65 mm, the bonding shear stress does not reach the peak value. The results show that the peak bonding shear stress is also transmitted to the free end, but its value is reduced gradually.

Figure 11 shows the relationship between the external load and the bonding shear stress (specimen T65). At the location of  $x = 170$  mm, the bonding shear stress reaches the maximum value 8.02 MPa when the specimen is loaded to 18 kN. At the location of  $x = 145$  mm, the peak bonding shear stress reaches 7.14 MPa when the load reaches to

**Table 3** Test results at different curing temperatures

Specimen number	Curing temperature (°C)	Cured time (h)	Ultimate load $P_{max}$ (kN)	Failure mode
T35	35	12	25.2	c
T40	40	12	29.5	b + c
T50	50	12	37.1	a + b + c
T60	60	12	36.3	a + b + c
T65	65	12	35.2	a + b + c

There are several types of failure modes [(a) CFRP strip fracture, (b) concrete–epoxy resin interface bond failure or adhesive cracking, (c) CFRP strip–epoxy resin interface bond failure]



**Fig. 8** Strain distribution of CFRP strip (T40)

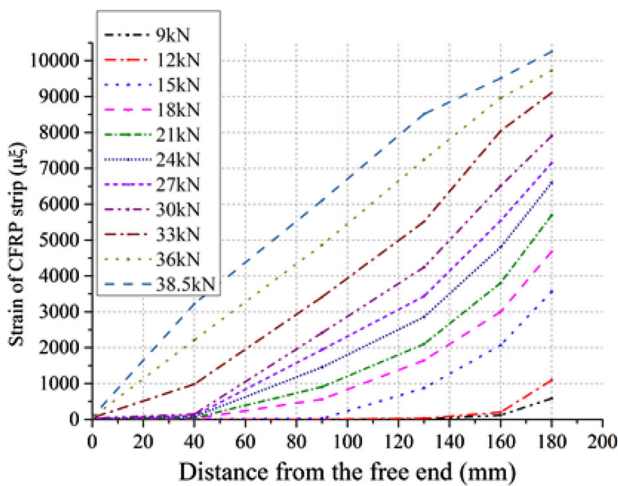


**Fig. 9** Strain distribution of CFRP strip (T50)

27 kN. As the load continues to increase, the bonding shear stress of the location of  $x = 65$  mm and  $x = 110$  mm also increases, but it does not reach the peak value when the specimen is damaged.

From the analysis results of Figs. 8, 9 and 10, the interfacial bonding shear stress between CFRP and concrete increases gradually with the increase in the external

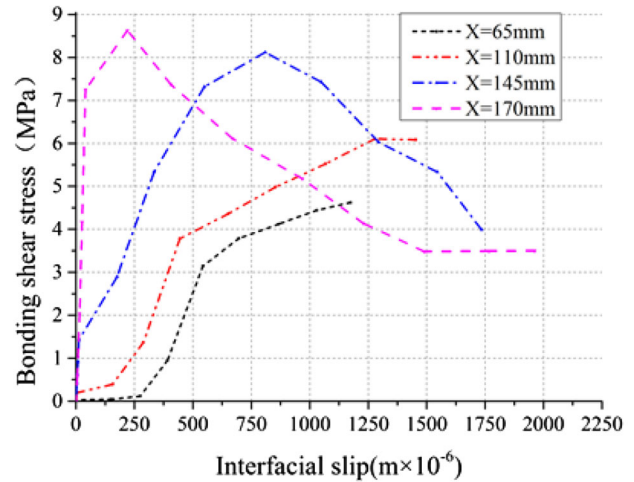


**Fig. 10** Bond–slip at different positions (T60)

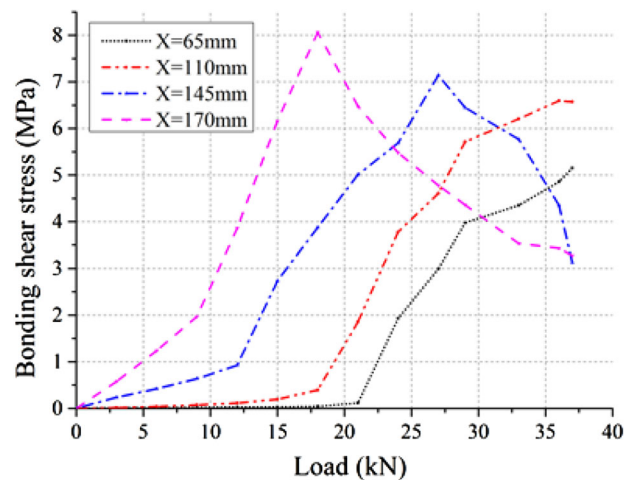


**Fig. 11** Load versus bonding shear stress at different positions (T65)

load acting on the specimens. The peak shear stress is gradually transmitted from the loading end to the free end.

Figure 12 shows the bond–slip curve of the loading end at different curing temperatures. With the increase in interface slip, the bonding shear stress first increases and then decreases. The peak bonding shear stress is related to the curing temperature. When curing temperature is 50 °C,

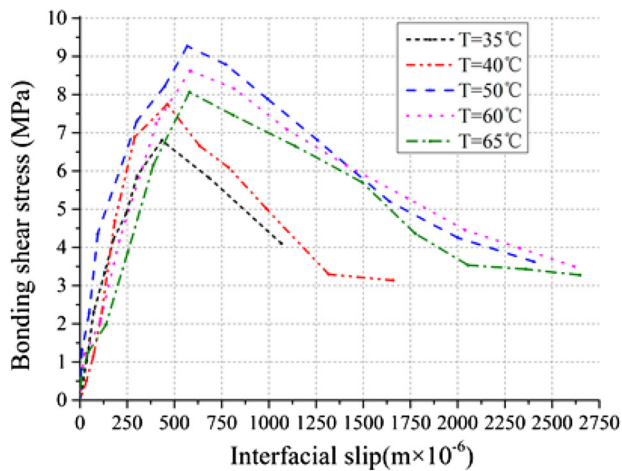


**Fig. 12** Bond–slip of loading end at different curing temperatures

the peak bonding shear stress reaches maximum value 9.17 MPa. In addition, with the increase in curing temperature, the change trend of bonding stiffness is basically consistent with peak shear stress.

According to the above analysis, curing temperature has a great influence on the bond performance of NSM CFRP strip. When its curing temperature is lower than glass transition temperature, the bond performance increases gradually with the curing temperature elevated. When it exceeds its glass transition temperature, the bond performance will gradually weaken with the increase in curing temperature.

### 3 Conclusions

In this paper, the influence of curing temperature is considered in the bond performance tests of NSM CFRP technique carried out by single shear pull-out methods. Through the pull-out experiments and analysis of test data, following conclusions are summarized.

- (1) With the increase in curing temperature, the strain of CFRP strip shows a relatively full trend with load changes. When curing temperature was less than 50 °C, the ultimate load increased gradually, which was increased by 47.2% from 35 to 50 °C. When curing temperature exceeded 50 °C, the ultimate load decreased gradually, which was reduced by 5% from 50 to 65 °C. With the increase in curing temperature, the ultimate load tends to first increase and then decrease. The failure modes were changed from CFRP strip–adhesive interface slip failure to broken CFRP strip. The bonding shear stress between CFRP and concrete gradually increases

with external load, which was transmitted from the loading end to the free end.

- (2) With the cure temperature increasing, the peak bonding shear stress first increases and then decreases. When curing temperature is 50 °C, the peak bonding shear stress reaches maximum value 9.17 MPa. In addition, the change trend of bonding stiffness is basically consistent with peak shear stress with the increase in curing temperature. Therefore, curing temperature of bonding materials has a great influence on the bond performance of NSM CFRP strip.
- (3) The overall research results mainly represent that the bonding performance of NSM CFRP specimens changes with the curing temperature, which can provide reference for the rapid reinforcement of monorail traffic track beams to select suitable curing temperature.

**Acknowledgements** This experiment was supported by research funds provided by China Railway Corporation Technology Research and Development Plan [Grant Number 2016G002-L] and Beijing Mass Transit Railway Operation Corporation Research Program [Grant Number 2016000501000005].

**Open Access** This article is distributed under the terms of the Creative Commons Attribution 4.0 International License (<http://creativecommons.org/licenses/by/4.0/>), which permits unrestricted use, distribution, and reproduction in any medium, provided you give appropriate credit to the original author(s) and the source, provide a link to the Creative Commons license, and indicate if changes were made.

### References

1. Rizkalla SH, Elhacha R (2004) Near-surface-mounted fiber-reinforced polymer reinforcements for flexural strengthening of concrete structures. *ACI Struct J* 101(5):717–726
2. Cruz JMS, Barros JAO (2004) Bond between near surface mounted carbon-fiber-reinforced polymer laminate strips and concrete. *J Compos Constr* 8(6):519–527
3. Hassan T, Rizkalla S (2003) Investigation of bond in concrete structures strengthened with near surface mounted carbon fiber reinforced polymer strips. *J Compos Constr* 7(3):248–356
4. Hassan T, Rizkalla S (2004) Bond mechanism of NSM FRP bars for flexural strengthening of concrete structures. *ACI Struct J* 101(6):830–841
5. Al-Mahmoud F, Castel A, Fran R, François R et al (2011) Anchorage and tension stiffening effect between near surface mounted CFRP rods and concrete. *Cement Concr Compos* 33(2):346–352
6. Seracino R, Nicola M (2007) Bond strength of near-surface mounted FRP strip-to-concrete joints. *J Compos Constr* 11(4):401–409
7. Sharaky IA, Torres L, Baena M et al (2013) An experimental study of different factors affecting the bond of NSM FRP bars in concrete. *Compos Struct* 99(5):350–365
8. Hu K, Dong K, Yang Y (2016) Temperature effect on bond behavior of carbon fiber reinforced polymer to concrete interface. *J Tongji Univ (Nat Sci Ed)* 06:845–852

9. Hu K, Lu F, Cai Z (2009) Researches on mechanical property of CFRP-concrete interface at elevated temperature. *J Tongji Univ (Nat Sci Ed)* 12:1592–1597
10. Lee H, Jung WT, Chung W (2017) Bond behavior of near surface mounted CFRP rods under temperature cycling. *Eng Struct* 137:67–75
11. Mohammed A, Al-Saadi NTK, Al-Mahaidi R (2016) Bond behaviour between NSM CFRP strips and concrete at high temperature using innovative high-strength self-compacting cementitious adhesive (IHSSC-CA) made with graphene oxide. *Constr Build Mater* 127:872–883
12. Yu B, Kodur V (2014) Effect of temperature on strength and stiffness properties of near-surface mounted FRP reinforcement. *Compos B Eng* 8(3):510–517
13. Capozucca R, Blasi MG, Corina V (2015) NSM technique: bond of CFRP rods and static/dynamic response of strengthened RC beams. *Compos Struct* 127:466–479